





ORIGINAL ARTICLE

A novel synaptopathy-defective synaptic vesicle protein trafficking in the mutant CHMP2B mouse model of frontotemporal dementia

Emma L. Clayton^{1,2}  | Katherine Bonnycastle^{3,4,5}  | Adrian M. Isaacs^{6,7} | Michael A. Cousin^{3,4,5}  | Stephanie Schorge¹ 

¹Department of Pharmacology, UCL School of Pharmacy, London, UK

²Currently at UK Dementia Research Institute at King's College London, London, UK

³Centre for Discovery Brain Sciences, University of Edinburgh, Edinburgh, Scotland

⁴Muir Maxwell Epilepsy Centre, University of Edinburgh, Edinburgh, Scotland

⁵Simons Initiative for the Developing Brain, University of Edinburgh, Edinburgh, Scotland

⁶UK Dementia Research Institute at UCL, London, UK

⁷Department of Neurodegenerative Disease, UCL Queen Square Institute of Neurology, London, UK

Correspondence

Emma L. Clayton, UK Dementia Research Institute at King's College London, London SE5 9RT, UK.

Email: emma.clayton@kcl.ac.uk

Funding information

This work was funded by the Wellcome Trust (S.S. and E.L.C.) (104033/Z/14/Z), Alzheimer's Research UK (E.L.C and S.S.) (PPG2018B-017) and the Simons Foundation (M.A.C. and K.B.) (529508). A.M.I. received funding from the European Research Council (ERC) under the European Union's Horizon 2020 research and innovation programme (648716 - C9ND), Alzheimer's Research UK, the Motor Neurone Disease Association and the UK Dementia Research Institute which receives its funding from DRI Ltd, funded

Abstract

Mutations in the ESCRT-III subunit CHMP2B cause frontotemporal dementia (FTD) and lead to impaired endolysosomal trafficking and lysosomal storage pathology in neurons. We investigated the effect of mutant CHMP2B on synaptic pathology, as ESCRT function was recently implicated in the degradation of synaptic vesicle (SV) proteins. We report here that expression of C-terminally truncated mutant CHMP2B results in a novel synaptopathy. This unique synaptic pathology is characterised by selective retention of presynaptic SV trafficking proteins in aged mutant CHMP2B transgenic mice, despite significant loss of postsynaptic proteins. Furthermore, ultrastructural analysis of primary cortical cultures from transgenic CHMP2B mice revealed a significant increase in the number of presynaptic endosomes, while neurons expressing mutant CHMP2B display defective SV recycling and alterations to functional SV pools. Therefore, we reveal how mutations in CHMP2B affect specific presynaptic proteins and SV recycling, identifying CHMP2B FTD as a novel synaptopathy. This novel synaptopathic mechanism of impaired SV physiology may be a key early event in multiple forms of FTD, since proteins that mediate the most common genetic forms of FTD all localise at the presynapse.

KEYWORDS

CHMP2B, endosome, ESCRT, frontotemporal dementia, lysosome, synaptic vesicle

Abbreviations: ADDB, activity dependent bulk endocytosis; CHMP2B, charged multivesicular body protein 2B; DIV, days in vitro; ESCRT, endosomal sorting complex required for transport; FTD, frontotemporal dementia; MVB, multivesicular body; ROI, region of interest; RP, reserve pool; RRP, readily releasable pool; SV, synaptic vesicle; Syp-pHluorin, synaptophysin-pHluorin.

This is an open access article under the terms of the Creative Commons Attribution License, which permits use, distribution and reproduction in any medium, provided the original work is properly cited.

© 2021 The Authors. *Journal of Neurochemistry* published by John Wiley & Sons Ltd on behalf of International Society for Neurochemistry.

by the UK Medical Research Council, Alzheimer's Society and Alzheimer's Research UK. This research was funded in whole, or in part, by the Wellcome Trust 104033/Z/14/Z. For the purpose of open access, the author has applied a CC BY public copyright licence to any Author Accepted Manuscript version arising from this submission.

1 | INTRODUCTION

Synaptopathies are disorders resulting from dysfunction of synapses and are associated with the earliest stages of multiple neuronal diseases. Synapse loss is a key feature in dementia, with synaptic dysfunction preceding neuronal death (Sheng et al., 2012; Terry, 2000). In Alzheimer's disease (AD), synapse degradation occurs before formation of amyloid deposits, and this degradation is the best correlate of cognitive decline in both animal models and AD patients (Dekosky & Scheff, 1990; Mucke et al., 2000; Serrano-Pozo et al., 2011; Terry et al., 1991). In frontotemporal dementia (FTD) patients have lower synaptic density in the superficial layers of the frontal cortex (Ferrer, 1999; Liu et al., 1996). However, it is not clear what is causing the damage to synapses in FTD, nor how this damage contributes to the clinical outcome for the disorder. The link is important because FTD is the second most common form of young-onset dementia (Harvey et al., 2003; Ratnavalli et al., 2002). FTD is characterised by atrophy of the frontal and temporal lobes that results in personality, behaviour and language changes (McKhann et al., 2001; Neary et al., 1998). Several genetic mutations cause FTD. Mutations in the genes that encode tau (*MAPT*), progranulin (*GRN*) and *C9orf72* are the most common, while additional rare mutations have been identified in valosin-containing protein (*VCP*), TDP-43 (*TARDBP*), fused in sarcoma (*FUS*) (Rohrer & Warren, 2011), TANK-binding kinase 1 (*TBK1*) (Gijssels et al., 2015; Le Ber et al., 2015; Pottier et al., 2015; van der Zee et al., 2017) and charged multivesicular body protein 2B (*CHMP2B*) (Lindquist et al., 2008; Skibinski et al., 2005).

A mutation in *CHMP2B*, found in a Danish cohort, causes an autosomal dominant form of FTD (Lindquist et al., 2008; Skibinski et al., 2005). The mutation disrupts a splice acceptor site and generates a C-terminally truncated variant of the protein. Physiological levels of this mutant *CHMP2B* are sufficient to recapitulate the patient phenotype in mice, producing axonal degeneration, gliosis and progressive neurodegeneration (Clayton et al., 2015, 2017; Gascon et al., 2014; Ghazi-Noori et al., 2012). The mechanism by which *CHMP2B*, a subunit of the endosomal sorting complex required for transport-III (ESCRT-III), causes these neurological deficits is not known. ESCRTs 0-III are highly conserved multi-subunit protein complexes that mediate numerous cellular processes involving scaffolding membrane deformation and budding (Vietri et al., 2020). Impaired endolysosomal trafficking is seen in primary cortical cultures from the mutant *CHMP2B* mouse model (Clayton et al., 2018), but the link between impaired endolysosomal trafficking and neuronal cell death is not well characterised.

Communication between neurons is reliant on the release of neurotransmitters from the presynaptic terminal through the fusion of synaptic vesicles (SVs) with the presynaptic plasma membrane. Maintaining the fidelity of neuronal communication depends on the efficient endocytosis of SV membrane and cargo components to sustain further rounds of exocytosis (Südhof, 2013). This finely tuned cycle is dependent on the action of a number of endocytosis proteins, and defects in this process have been implicated in numerous neurodevelopmental and neurodegenerative conditions (Bonnycastle et al., 2020; Melland et al., 2020). Different modes of SV retrieval with characteristic molecular requirements have been described, and are known to be activated by different stimulation paradigms; clathrin-mediated endocytosis, kiss-and-run, activity dependent bulk endocytosis (ADBE) and ultrafast endocytosis have all been reported at central nerve terminals (Chanaday et al., 2019). While molecular mechanisms that control SV endocytosis have been described, little is known about the process by which SV proteins are trafficked for degradation. Interestingly, the ESCRT complex was recently implicated in the degradation of a subset of SV proteins (Sheehan et al., 2016). However, the impact of mutation in the ESCRT subunit *CHMP2B* on SV physiology is unknown.

We show that mutant *CHMP2B* leads to synaptic loss, and a concurrent retention of SV-associated proteins in aged *CHMP2B* mice. Presynaptic endosomes are significantly increased in mutant *CHMP2B* primary cortical neurons. In neurons expressing mutant *CHMP2B* the total recycling pool of SVs is increased, fewer SVs fuse during a defined stimulus and SV endocytosis starts to fail when the system is stressed. Thus, we report here that defects in SV protein physiology caused by mutant *CHMP2B* affect presynaptic SV trafficking, leading to synaptopathy in *CHMP2B* FTD.

2 | MATERIALS AND METHODS

2.1 | Mice

All experimental procedures were carried out in accordance with the UK Animals (Scientific Procedures) Act 1986.

At Edinburgh work was carried out under Project and Personal Licence authority approved by the local Animal Welfare and Ethical Review Body (Home Office project licence—7008878). Animals were killed by schedule 1 procedures in accordance with UK Home Office Guidelines. Adults were killed by exposure to rising levels of CO₂ followed by dislocation of neck, embryos were killed by decapitation

followed by destruction of the brain. Mice were housed in conventional caging.

At UCL mouse work was performed under UK government Home Office project licence 7009014, approved by local Animal Welfare and Ethical Review Body. Mice were housed in a category 3 SPF facility in individually ventilated cages under negative pressure in groups of 3–5 animals with environmental condition targets of temperature $20 \pm 2^\circ\text{C}$, relative humidity $55\% \pm 10\%$, 12:12 hour photo period. Mice were provided with water and pelleted diet ad lib. All cages are provided with environmental enrichment in the form of nesting material, chew blocks and mouse houses.

The previously described mutant CHMP2B^{Intron5} expressing mouse line Tg153 (Ghazi-Noori et al., 2012) was backcrossed over 10 generations to C57Bl6J and was maintained as a homozygous line.

2.2 | Whole brain homogenates

10% (w/v) brain homogenates (minus the cerebellum and olfactory bulb) were prepared in phosphate-buffered saline containing complete EDTA-free protease inhibitors (Roche) using a TissueRuptor (Qiagen) to make a 10% w/v solution and combined 1:1 with 2% sarkosyl (N-lauroylsarcosine) in D-PBS. Benzonase (50 U/ml; Novagen) was added to remove DNA and the homogenates incubated with constant agitation at 37°C for 1 h, followed by ultracentrifugation at $100\,000\text{ g}$ for 30 min at 4°C . $2\times$ Laemmli sample buffer was added to the supernatant and heated at 100°C for 10 min prior to sodium dodecyl sulphate-polyacrylamide gel electrophoresis.

2.3 | Immunoblotting

Samples were run on NuPAGE 4–12% Bis-Tris gel electrophoresis gels (Invitrogen) with NuPAGE MOPS buffer then transferred onto nitrocellulose using a TransBlot turbo system (Bio-Rad). Total protein loading was assayed using Revert Total Protein Stain kit (LiCor). Membranes were blocked for 1 h at room temperature with 5% milk/PBS-T and probed with primary antibodies (see Table 1) overnight at 4°C in 1% milk/PBS-T with constant agitation. Detection was

performed with anti-mouse and anti-rabbit-IRDye 680 and 800CW (LiCor), 1:10 000 fluorescent secondary antibodies for visualisation using a LiCor Odessey scanner. Quantification was performed using Licor software, bands were normalised to total protein loading, and averages were taken of three mice per genotype.

2.4 | Primary cortical cultures

Primary cortical cultures were prepared from mixed sex mice (post-natal day 0 or day 1), with 3 mice used per culture. Mice were euthanised by decapitation. Briefly, the cortices were dissected, pooled, digested in trypsin (Sigma) and triturated with a fine fire polished Pasteur pipette to achieve a single cell suspension. Cells were plated in a minimal volume of Dulbecco's Modified Eagle's Medium supplemented with 10% fetal bovine serum, 1% penicillin/streptomycin and 1% Glutamax (all Invitrogen), at a density of 1000 cells/ mm^2 on coverslips coated with poly-D-lysine (Sigma). 1–2 h after plating, maintenance medium of Neurobasal A containing 2% B27, 0.25% penicillin/streptomycin and 0.25% Glutamax (all Invitrogen) was added to the cells. Neurons were cultured at 37°C and 5% CO_2 .

2.5 | Electron microscopy

Primary cortical cultures were plated in Permaxox slide chambers (VWR International). At 14 days in vitro cultures were either immediately fixed for rest condition, stimulated with warm modified tyrodes solution (90 mM NaCl, 64 mM KCl, 2 mM MgCl_2 , 10 mM glucose, 10 mM HEPES, 2 mM CaCl_2) before fixation for stimulated condition, or incubated for 5 min after stimulation before fixation for recovery condition.

Samples were fixed in 3% EM grade glutaraldehyde (Agarscientific.com) in 0.1 M sodium cacodylate (Agarscientific.com) and 5 mM CaCl_2 pH7.4. Samples were washed in dH_2O before 2 h in 1% $\text{OsO}_4(\text{aq})$ (Agarscientific.com). Following a wash with dH_2O , samples were washed for 10 min each in a series of 70% ethanol, 90% ethanol and finally 4 times in 100% absolute ethanol. Samples were washed twice in propylene oxide for 15 min before the addition of

Antibody	Company	Catalogue number	Dilution
Actin	Sigma	A5441	1:10 000
Amphiphysin	Synaptic Systems	120 002	1:1000
Endophilin	Synaptic Systems	159 002	1:1000
Homer	Synaptic Systems	160 008	1:1000
MUNC-18	Synaptic Systems	116 002	1:1000
PSD-95	Genetex	6G6-IC9	1:1000
Synapsin 1/2	Synaptic Systems	106 002	1:1000
Syntaxin 1A	Synaptic Systems	110 302	1:1000
Synuclein	University of Iowa Hybridoma Bank	H3C	1:1000

TABLE 1 Primary antibodies for western blotting

a 1:1 propylene oxide/araldite resin mixture for 60 min. Samples were placed in a neat araldite resin mixture overnight in fresh vials on a slow rotator and embedded the next day in neat araldite resin mixture. Polymerisation proceeded for 2–3 days in a 60°C oven. Semithin sections were cut at 1 µm and stained with toluidine blue, with ultrathin sections cut at 50–70 nm, collected on 300 mesh copper grids and stained with saturated methanolic uranyl acetate and Reynolds Lead citrate.

2.6 | Syp-pHluorin assay

Cortical neurons were prepared as above with the following modifications; cultures were prepared from embryonic day 16.5–17.5 mice and cells plated at 70 000 cells per coverslip. 6–8 mice were used per culture. Cultures were transfected with 0.5 µg CHMP2B WT or mutant CHMP2B and 1 µg syp-pHluorin (provided by Prof. L. Lagnado, University of Sussex) 24 h prior to imaging using Lipofectamine 2000 as per manufacturer's instructions. Transfected neurons were visualised at 500 nm band pass excitation with a 515 nm dichroic filter and a long-pass >520 nm emission filter on a Zeiss Axio Observer D1 inverted epifluorescence microscope (Cambridge). Images were captured using an AxioCam 506 mono camera (Zeiss) with a Zeiss EC Plan Neofluar 40x/1.30 oil immersion objective. Cortical cultures were mounted in a Warner Instruments imaging chamber with embedded parallel platinum wires (RC21BRFS) and challenged with field stimulation using a Digitimer LTD MultiStim system-D330 stimulator (current output 100 mA, current width 1 ms). Imaging time courses were acquired at 4 s intervals using Zen Pro software (Zeiss) while undergoing constant perfusion with imaging buffer (119 mM NaCl, 2.5 mM KCl, 2 mM CaCl₂, 2 mM MgCl₂, 25 mM HEPES, 30 mM glucose at pH 7.4), with 10 µM 6-cyano-7-nitroquinoxaline-2,3-dione (CNQX) and 50 µM DL-2-Amino-5-phosphonopentanoic acid (AP-5). NH₄Cl alkaline buffer (50 mM NH₄Cl substituted for 50 mM NaCl) was used to reveal the maximal pHluorin response. Time traces were analysed using the Fiji distribution of Image J (National Institutes of Health). Images were aligned using the Rigid body model of the StackReg plugin (<https://imagej.net/StackReg>). Nerve terminal fluorescence was measured using the Time Series Analyser plugin (<https://imagej.nih.gov/ij/plugins/time-series.html>). Regions of interest (ROIs) 5 pixels in diameter were placed over nerve terminals that responded to the first electrical stimulus. A response trace was calculated for each cell by averaging the individual traces from each selected ROI. For all experiments *n* is the number of coverslips imaged across three independent cortical preparations.

2.7 | Statistics

Statistical analyses were performed in Graphpad. Statistical tests and *N* numbers are indicated in the figure legends and were used to calculate significance values with **p* < 0.05, ***p* < 0.01, ****p* < 0.001,

****p* < 0.0001. Western blot data were not assessed for normality because of low sample size. Electron microscopy data were assessed for normality using the Shapiro-Wilk normality test. Sample size calculations were not performed, and *N* numbers were based on previous studies of a similar nature (Clayton et al., 2015, 2018; Nicholson-Fish et al., 2015). Comparisons between non-transgenic and mutant CHMP2B cultures were performed by a researcher blinded to sample origin.

2.8 | Study design

This study was not pre-registered, randomisation was not performed to allocate treatments to different experimental groups, no exclusion criteria were pre-determined, no test for outliers was performed, and the study was exploratory.

3 | RESULTS

3.1 | Reduction of postsynaptic, but not presynaptic proteins in aged CHMP2B mutant mice

The ESCRT complex was recently implicated in the degradation of presynaptic SV proteins (Sheehan et al., 2016); however, it is not known if mutation in CHMP2B disrupts this highly specialised membrane trafficking pathway. Characteristic FTD-like pathology is well established at 18 months in mutant CHMP2B mice, with significant accumulation of p62, ubiquitin and lysosomal storage related aggregates (Clayton et al., 2015; Ghazi-Noori et al., 2012). We have reported significant cortical volume loss, despite established gliosis, in aged mutant CHMP2B mouse brains, which is because of significant neuronal loss (Clayton et al., 2017).

In order to determine whether mutant CHMP2B has an effect on presynapses, we first investigated the levels of pre- and post-synaptic proteins. As expected, there was a significant reduction in the postsynaptic markers PSD-95 (control 1.00 ± 0.07, CHMP2B^{Intron5} 0.77 ± 0.04, *p* = 0.02) and Homer (control 1.00 ± 0.04, CHMP2B^{Intron5} 0.84 ± 0.02, *p* = 0.01) in aged mutant CHMP2B mice (Figure 1a), consistent with the neuronal loss previously reported in these mice at 18 months (Clayton et al., 2017). However, surprisingly no difference was seen in the levels of several presynaptic SV-associated proteins in mutant CHMP2B compared to age-matched non-transgenic controls (Figure 1b). Mutant CHMP2B mice do not show a significant decrease in levels of Amphiphysin (control 1.00 ± 0.03, CHMP2B^{Intron5} 1.04 ± 0.06, *p* = 0.26), Synapsin (control 1.00 ± 0.03, CHMP2B^{Intron5} 0.94 ± 0.04, *p* = 0.18) or Endophilin (control 1.00 ± 0.003, CHMP2B^{Intron5} 0.94 ± 0.04, *p* = 0.12), and in fact show a significant increase in the amount of Synuclein (control 1.00 ± 0.04, CHMP2B^{Intron5} 1.26 ± 0.05, *p* = 0.005) (Figure 1b). This result was surprising, as we expected to see a concurrent loss of markers of both the pre- and post-synaptic compartment because of the known neuronal loss at 18 months in this model (see Table 2).

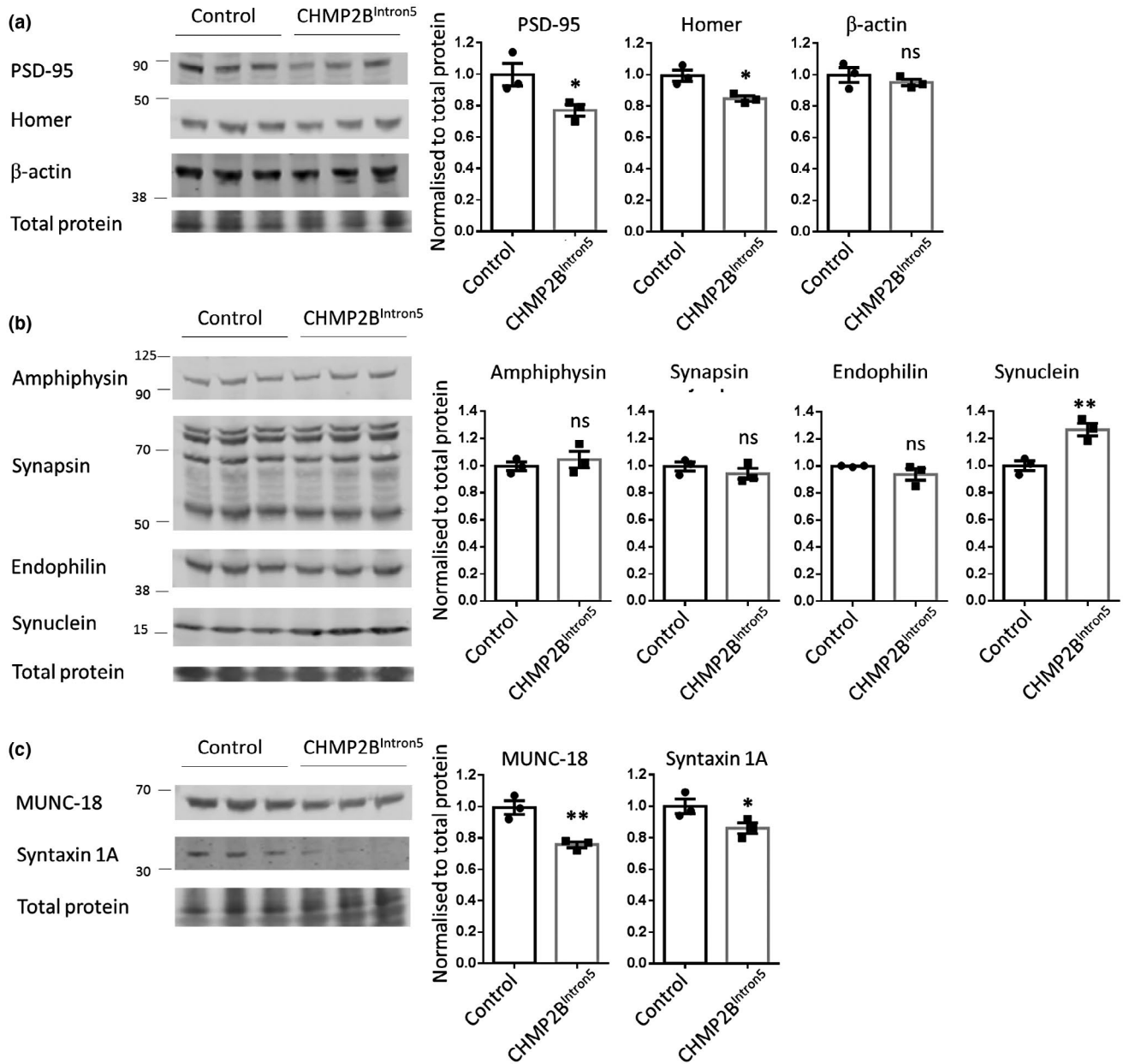


FIGURE 1 Reduction of postsynaptic and select presynaptic proteins in aged CHMP2B mutant mice. Brain homogenates from 18-month-old CHMP2B^{Intron5} and non-transgenic female mice were extracted in 1% sarkosyl and immunoblotted for markers of the postsynaptic and presynaptic compartments. The amount of PSD-95 and Homer (a) in CHMP2B^{Intron5} brain homogenates is significantly reduced when compared to non-transgenic controls. Brain homogenates were additionally immunoblotted for Amphiphysin, Synapsin, Endophilin and Synuclein (b). No significant difference was seen between non-transgenic and CHMP2B^{Intron5} mice for Amphiphysin, Synapsin or Endophilin, while Synuclein was significantly increased in aged mutant CHMP2B homogenates. Brain homogenates were also immunoblotted for MUNC-18 and Syntaxin 1A (c), which were significantly decreased in aged mutant CHMP2B mouse brain. Mean ± SEM is shown. Unpaired t-test, * $p < 0.05$, ** $p < 0.01$, ns = not significant. $N = 3$ mice of each genotype

3.2 | Aged CHMP2B mutant mice specifically retain a subset of SV trafficking proteins

To test whether the observed retention of SV-associated proteins was because of the selective preservation of entire presynaptic units, despite observed loss of markers of the postsynaptic compartment, we blotted for additional presynaptic components. MUNC-18

and Syntaxin 1A localise to the plasma membrane of the presynaptic terminal, and mediate tethering of SVs for fusion events, but do not participate in SV recycling (Kavanagh et al., 2014). These presynaptic components were significantly decreased in mutant CHMP2B mouse brain (MUNC-18 control 1.00 ± 0.04 , CHMP2B^{Intron5} 0.76 ± 0.02 , $p = 0.004$, Syntaxin 1A control 1.00 ± 0.05 , CHMP2B^{Intron5} 0.86 ± 0.03 , $p = 0.036$) (Figure 1c), suggesting that the observed

TABLE 2 Summary of statistics

Figure 1		p value	t, df	
PSD-95	Unpaired t-test, one-tailed	0.0242	t = 2.809 df = 4	
Homer	Unpaired t-test, one-tailed	0.0102	t = 3.719 df = 4	
Actin	Unpaired t-test, one-tailed	0.2064	t = 0.9133 df = 4	
Amphiphysin	Unpaired t-test, one-tailed	0.2557	t = 0.7200 df = 4	
Synapsin	Unpaired t-test, one-tailed	0.1818	t = 1.024 df = 4	
Endophilin	Unpaired t-test, one-tailed	0.1215	t = 1.369 df = 4	
Synuclein	Unpaired t-test, one-tailed	0.0051	t = 4.581 df = 4	
MUNC-18	Unpaired t-test, one-tailed	0.0037	t = 5.020 df = 4	
Syntaxin 1A	Unpaired t-test, one-tailed	0.0357	t = 2.437 df = 4	
Figure 2		p value		
Endosomes rest	Mann-Whitney test	<0.0001		
SVs rest	Mann-Whitney test	0.9985		
Endosomes stimulated	Mann-Whitney test	<0.0001		
SVs stimulated	Mann-Whitney test	0.0619		
Endosomes recovery	Mann-Whitney test	0.0015		
SVs recovery	Mann-Whitney test	0.4684		
Figure 3				
SypHy $\Delta F/F_0$	Two-way ANOVA			
ANOVA table	DF	MS	F (DFn, DFd)	p value
Interaction	3	0.01037	F (3, 88) = 0.2895	p = 0.8329
Bonferroni's multiple comparisons test	95% CI of diff.	Significant?	Summary	Adjusted p Value
Peak 1	0.02591 to 0.4213	Yes	*	0.0197
Peak 2	-0.04672 to 0.3486	No	ns	0.2187
Peak 3	-0.06861 to 0.3267	No	ns	0.3979
Peak 4	-0.05055 to 0.3448	No	ns	0.2439
SypHy $\Delta F/F_0$ (Normalised to stim 1)	Two-way ANOVA			
ANOVA table	DF	MS	F (DFn, DFd)	p value
Interaction	3	0.0114	F (3, 88) = 0.4416	p = 0.7239
Bonferroni's multiple comparisons test	95% CI of diff.	Significant?	Summary	Adjusted p Value
Peak 1	-0.1679 to 0.1679	No	ns	>0.9999
Peak 2	-0.1516 to 0.1841	No	ns	>0.9999
Peak 3	-0.1855 to 0.1502	No	ns	>0.9999
Peak 4	-0.08534 to 0.2504	No	ns	0.8533
SypHy $\Delta F/F_0$ @ 120s	Two-way ANOVA			
ANOVA table	DF	MS	F (DFn, DFd)	p value
Interaction	3	0.0488	F (3, 88) = 0.9281	p = 0.4307
Bonferroni's multiple comparisons test	95% CI of diff.	Significant?	Summary	Adjusted p Value
Peak 1	-0.2965 to 0.1825	No	ns	>0.9999
Peak 2	-0.3465 to 0.1325	No	ns	>0.9999
Peak 3	-0.4204 to 0.05869	No	ns	0.2297
Peak 4	-0.5042 to -0.02510	Yes	*	0.0239
Figure 4		p value	t, df	
RRP	Unpaired t-test, two-tailed	0.0582	t = 2.031 df = 17	

TABLE 2 (Continued)

Recycling pool	Unpaired <i>t</i> -test, two-tailed	0.0424	<i>t</i> = 2.194 df = 17
Reserve pool	Unpaired <i>t</i> -test, two-tailed	0.082	<i>t</i> = 1.849 df = 17
Resting pool	Unpaired <i>t</i> -test, two-tailed	0.3939	<i>t</i> = 0.8747 df = 17
Total pool	Unpaired <i>t</i> -test, two-tailed	0.0859	<i>t</i> = 1.823 df = 17

retention of SV-associated presynaptic proteins in mutant CHMP2B mouse brain may be restricted to components of SV endocytosis, and not extend to all parts of the presynaptic terminal.

No alteration to postsynaptic or presynaptic components was observed at 6 months of age in mutant CHMP2B mouse brains (Figure S1). This shows that these changes are a result of an ongoing degenerative process and not a developmental defect.

These data show that SV trafficking components are selectively retained in aged mutant CHMP2B mouse brain. In conjunction with the recent observation that the ESCRT complex mediates degradation of SV components (Sheehan et al., 2016), this led us to investigate the physiology of SV trafficking in mutant CHMP2B neurons.

3.3 | Mutant CHMP2B synapses are characterised by increased number of presynaptic endosomes

We reasoned that this increase in a subset of SV proteins may indicate an alteration to SV trafficking pathways. To assess this, we used electron microscopy to examine the ultrastructure of the presynaptic SV pool in primary cortical cultures to determine whether evidence of dysfunction was apparent.

We analysed synapses of mature primary cortical mutant CHMP2B or wildtype cultures at 14 days *in vitro* (DIV). We initially quantified the number of SVs and presynaptic endosomes per synaptic terminal in unstimulated cultures (Figure 2a). SVs were readily identified because of their uniform size of approximately 50 nm. Structures over 50 nm in diameter (measured at the widest point) were designated as endosomes. Mutant CHMP2B cultures contained significantly more presynaptic endosomes per terminal when compared to controls (control 0.54 ± 0.09 , CHMP2B^{Intron5} 1.21 ± 0.19 , $p = 0.0007$) (Figure 2b). No significant difference was seen in the number of SVs per terminal (control 43.32 ± 2.78 , CHMP2B^{Intron5} 42.58 ± 3.12 , $p = 0.86$) (Figure 2c).

Since nerve terminal stimulation dynamically alters the proportion of SVs and endosomes in the short term (as SVs fuse and then get retrieved by different endocytosis modes), we next examined the effects of stimulation on the presynaptic ultrastructure. Cultures were stimulated to turn over the maximum amount of SV membrane and then fixed immediately (Figure 2d). The number of presynaptic endosomes per mutant CHMP2B terminal was found to be significantly further increased over control terminals (control 0.89 ± 0.14 , CHMP2B^{Intron5} 2.88 ± 0.26 , $p < 0.0001$) (Figure 2e).

Defects in trafficking either to or from the presynaptic endosome could drive the observed ultrastructural defects at the presynaptic

terminal. Strong stimulation of the presynaptic terminal stimulates ADBE, a specialised endocytic event whereby a large membrane invagination retrieves membrane sufficient for several SVs (Clayton et al., 2009, 2010). To investigate if this process is up-regulated in mutant CHMP2B neurons, large fluorescent dextran was applied to primary cortical cultures during strong stimulation. Labelled dextran is too large to be internalised during single SV reformation events, and thus is a selective marker for larger infoldings of membrane characteristic of ADBE (Clayton et al., 2008). Co-localisation of fluorescent dextran with the presynaptic marker SV2 was used to quantify the proportion of synapses that had activated ADBE following strong stimulation (Figure S2). No significant difference in the proportion of SV2 positive puncta containing fluorescent dextran was seen when mutant CHMP2B neurons were compared to control neurons. Thus, the increase seen in the number of endosomes at mutant CHMP2B presynaptic terminals does not occur because of an up-regulation of ADBE.

Following stimulation, SV pools are replenished by clathrin-mediated endocytosis which persists at both the plasma membrane and endosomes after stimulation (Clayton et al., 2008; Kononenko et al., 2014; Watanabe et al., 2014). To determine the role of mutant CHMP2B on replenishment of SV pools, we investigated the reformation of the SV pool after depletion by stimulation. Cultures were fixed 5 min after the end of strong stimulation, when the majority of SVs will normally have recycled to their respective vesicle pools (Figure 2g). As expected, the number of endosomal structures in the mutant CHMP2B presynaptic terminals remained significantly greater following 5 min of recovery (control 0.45 ± 0.09 , CHMP2B^{Intron5} 1.05 ± 0.18 , $p = 0.0024$) (Figure 2h). However, no significant difference in the number of SVs was detected (control 39.44 ± 2.13 , CHMP2B^{Intron5} 36.33 ± 2.32 , $p = 0.35$) (Figure 2i). In addition, no significant difference in the diameter of the presynaptic endosomes was seen in any of the conditions assessed (Figure S3). Therefore, the increased number of endosomes was not because of stalled SV generation from these structures. Although ESCRTs are important for formation of multivesicular bodies (MVBs), no difference was seen in the number of MVBs seen per synapse (Figure S4).

Therefore, our ultrastructural analysis of mutant CHMP2B presynaptic anatomy reveals an increased number of endosomes in resting CHMP2B nerve terminals. This increase was not because of ADBE, since generation of endosomes directly from the presynaptic membrane is unaffected by the presence of mutant CHMP2B. Instead, there appears to be a permanent increase in presynaptic endosomes, as evidenced by their sustained increase above baseline levels following stimulation.

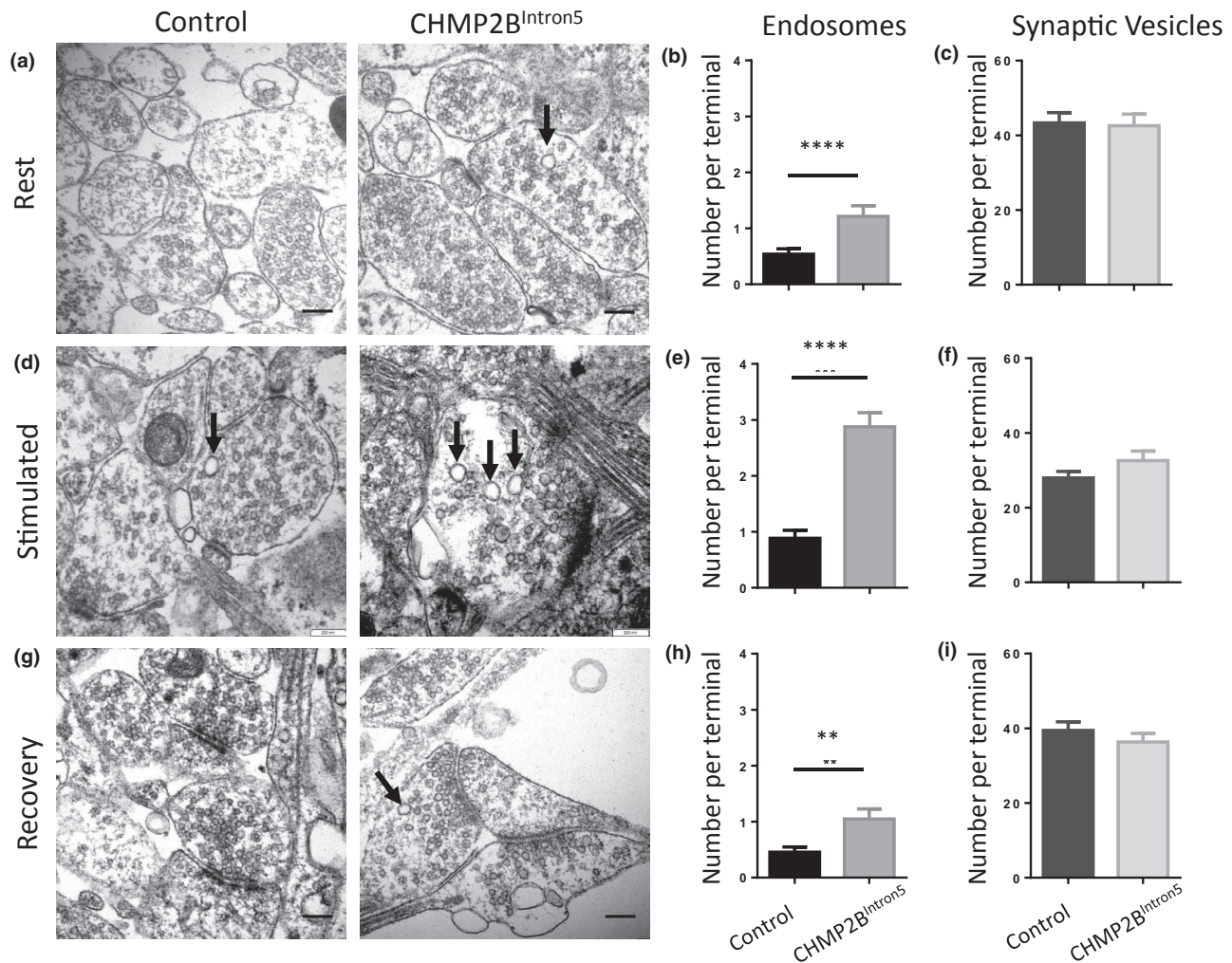


FIGURE 2 Presynaptic endosome defects in mutant CHMP2B primary cortical cultures. (a) Representative images of non-transgenic or CHMP2B^{Intron5} presynaptic structures fixed at rest in DIV 14 primary cortical cultures. The number of endosomes (b) and synaptic vesicles per synapse (c) were quantified. (d) Representative images of cultures fixed immediately following a 2 min strong stimulation. (e) Quantification of the average number of endosomes and synaptic vesicles (f) per presynapse following strong stimulation. (g) Cultures were allowed to rest for 5 min following strong stimulation, then fixed. (h) The average number of endosomes and synaptic vesicles (i) following recovery was quantified. Mann-Whitney test, ** $p < 0.01$, **** $p < 0.0001$, Mean \pm SEM is shown. Rest $n = 117$ non-transgenic synapses and 84 CHMP2B^{Intron5}, Stim $n = 113$ non-transgenic synapses and 48 CHMP2B^{Intron5} synapses, Recovery $n = 86$ non-transgenic synapses and 64 CHMP2B^{Intron5} synapses. Arrows indicate examples of presynaptic endosomes. Scale bar 200 nm

3.4 | SV exocytosis is significantly impaired in mutant CHMP2B primary cultures

The increased number of endosomes within CHMP2B mutant nerve terminals, in conjunction with retention of select presynaptic SV proteins, suggests dysfunction in the clearance of SV proteins by the endolysosomal system. To determine whether this impacted the dynamics of SV turnover, we co-transfected primary cultures with CHMP2B constructs and a genetically encoded fluorescent reporter of SV trafficking called pHluorins. These reporters are SV cargoes linked to a luminal pH-sensitive EGFP, allowing them to fluoresce when at the plasma membrane but their fluorescence is quenched when SVs reacidify following endocytosis (Kavalali & Jorgensen, 2014). Fluorescence quenching can be used as an estimate of the

speed of SV cargo retrieval, as the endocytosis of SVs is rate limiting compared to SV acidification (Atluri & Ryan, 2006; Egashira et al., 2015).

Mutant and wildtype CHMP2B expressing neurons that co-expressed syp-pHluorin were challenged with repeated trains of 400 action potentials (40 Hz for 10 seconds). This protocol reveals both acute perturbations in SV recycling and also accumulated defects because of disrupted endolysosomal trafficking (Nicholson-Fish et al., 2015). From first stimulation, significantly less SV exocytosis (reported as evoked peak pHluorin response) occurred in neurons expressing mutant CHMP2B compared to wildtype CHMP2B (wildtype $0.596 \pm 0.085 \Delta F/F_0$, mutant 0.373 ± 0.048 , $p = 0.02$ two-way ANOVA, Figure 3a,b). This pattern was repeated for each subsequent neuronal stimulation. Interestingly, when the fluorescence

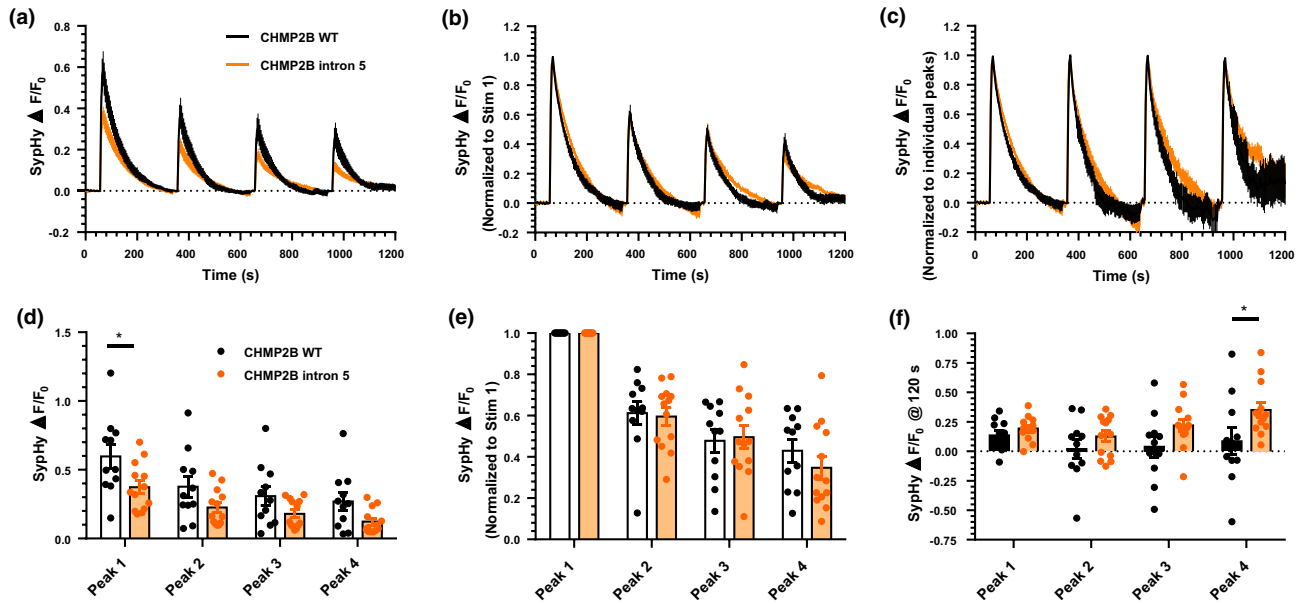


FIGURE 3 Defective exocytosis in mutant CHMP2B expressing neurons. Cortical neurons derived from WT mice were transfected with CHMP2B^{Wildtype} or CHMP2B^{Intron5} and sypHy 24 h prior to imaging and imaged day *in vitro* (DIV) 13–14. Transfected neurons were stimulated four times with action potential trains (40 Hz 10 s) at 5 min intervals. a,c,e, Mean traces displaying the average sypHy fluorescent response traces ($\Delta F/F_0$) of cortical neurons expressing CHMP2B^{Wildtype} (black) and CHMP2B^{Intron5} (orange) displayed \pm SEM. Average traces display $\Delta F/F_0$ (a), the peak sypHy response normalised to the first action potential train (c) and the peak sypHy response normalised to each action potential train (e). (b, d) Mean sypHy peak heights for (a) and (c), 2-way ANOVA $*p < 0.05$. (f) Normalised sypHy fluorescence 120 s after each stimulation. For all experiments, $n = 11$ for CHMP2B^{Wildtype} and $n = 13$ for CHMP2B^{Intron5}

peaks are normalised to the initial response, there is no accumulated defect in SV exocytosis between wildtype and mutant CHMP2B neurons (Figure 3c,d). The absence of an accumulated defect may relate to the relative increase in the population of presynaptic molecules in mutant CHMP2B neurons that are able to sustain exocytosis, albeit at a reduced level. Interestingly, when the recovery of the pFluorin response was examined after each action potential train, SV endocytosis was unaffected in CHMP2B mutant neurons until the final stimulus (wildtype $0.085 \pm 0.113 \Delta F/F_0$ at 120 sec, mutant 0.350 ± 0.061 , $p = 0.024$ two-way ANOVA, Figure 3e,f). Therefore, mutant CHMP2B expressing neurons have no intrinsic defect in SV endocytosis; however, a fragility in this response is revealed over the course of the sequential stimulations.

3.5 | Increased recycling pool mobilisation in mutant CHMP2B expressing neurons

SVs reside in different pools in the presynaptic terminal, the recycling or the resting pool. The recycling pool of SVs is responsive to evoked stimulation, while the resting pool is resistant to exocytic stimuli (Chanaday et al., 2019; Kim & Ryan, 2010). Recycling SVs can be further subdivided into the readily releasable pool (RRP), where SVs are docked at the presynaptic terminal, and the reserve pool (RP), from which SVs are mobilised during periods of intense activity (Chanaday et al., 2019) (Figure 4a). The observed decrease in SV exocytosis in CHMP2B neurons may be a result of less SVs

fusing, or redistribution of SVs between functional pools. To investigate this, differing stimulation paradigms that mobilise different pools of SVs in pFluorin-transfected neurons were applied. Pool size was estimated in primary cortical cultures treated with the V-type ATPase inhibitor bafilomycin A1, which isolates SV exocytosis from endocytosis (Sankaranarayanan & Ryan, 2001). Cultures were stimulated with two trains of action potentials, 20 Hz for 2 s (to reveal the readily releasable pool, RRP) and 20 Hz 80 s to reveal the reserve pool (RP) (Figure 4b). The values together represent the total recycling pool of SVs. Interestingly, the recycling pool of SVs is significantly greater in mutant CHMP2B expressing neurons (wildtype $0.382 \pm 0.069 \Delta F/F_0$, mutant 0.690 ± 0.130 , $p = 0.042$, students unpaired *t*-test, Figure 4d).

To obtain the resting pool values, the recycling pool fluorescence (summed RRP and RP fluorescence) was subtracted from total fluorescence (revealed by alkaline buffer perfusion) (wildtype $0.409 \pm 0.075 \Delta F/F_0$, mutant 0.510 ± 0.086 , $p = 0.394$, students unpaired *t*-test Figure 4f). The large but non-significant increase in the total pool in mutant CHMP2B expressing neurons (wildtype $0.791 \pm 0.114 \Delta F/F_0$, mutant 1.200 ± 0.211 , $p = 0.086$, students unpaired *t*-test Figure 4g) may occur as a result of a block in endolysosomal trafficking.

Taken together, these results show that fewer SVs fuse during a defined stimulus and SV endocytosis starts to fail when the system is stressed. Additionally, the total recycling pool of SVs is increased in mutant CHMP2B expressing neurons- this may occur as a compensatory mechanism to the endolysosomal block.

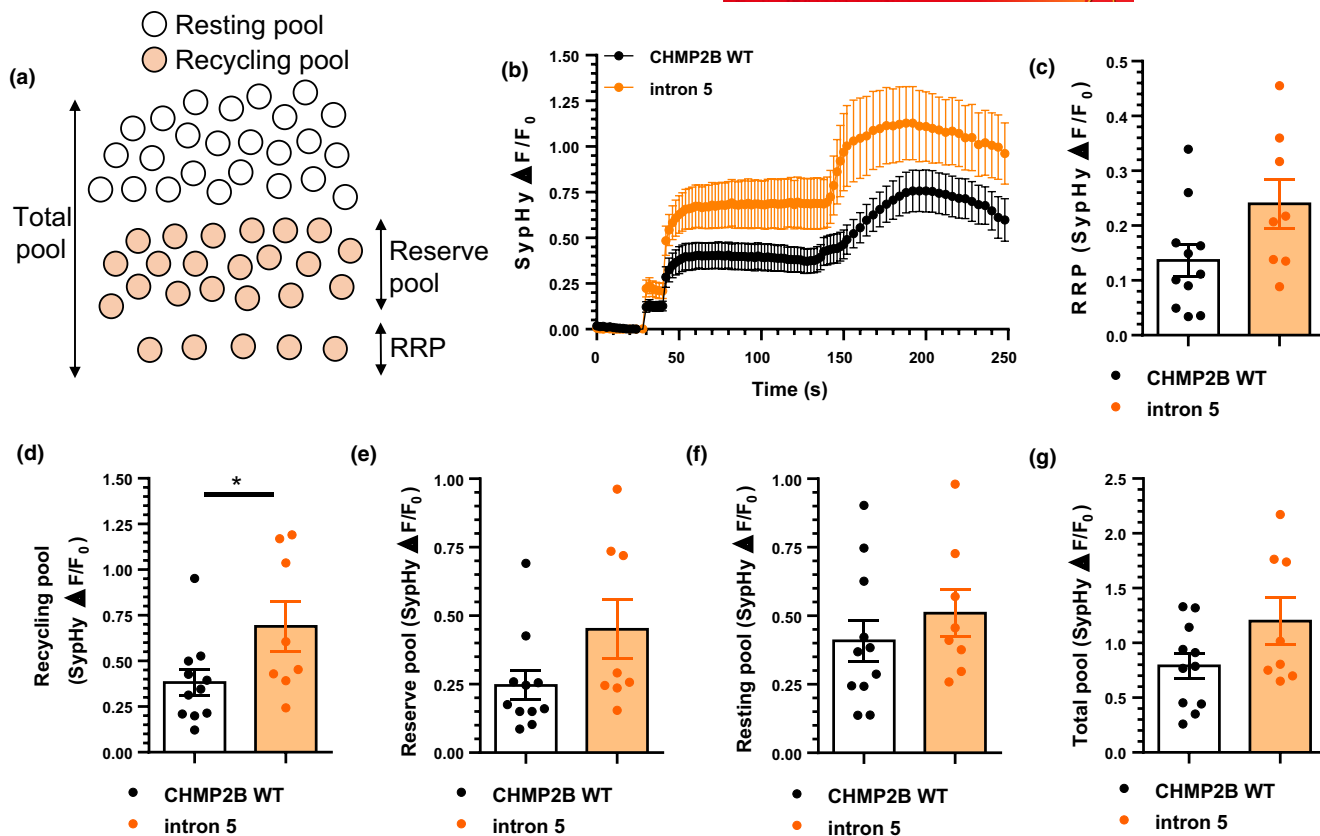


FIGURE 4 Increased recycling pool mobilisation in mutant CHMP2B expressing neurons. (a) Schematic of SV pool organisation. The total SV pool is comprised of the resting pool (cannot be mobilised by action potentials, revealed by NH_4Cl) and the recycling pool. The recycling pool can be subdivided into the RRP (20 Hz 2 s) and reserve pool (20 Hz 80 s). Cortical neurons derived from WT mice were transfected with CHMP2B^{Wildtype} or CHMP2B^{Intron5} and syHy 24 h prior to imaging and imaged DIV 13–14 in the presence of 1 μM Bafilomycin A1. Transfected neurons were challenged with two trains of action potentials (20 Hz, 2 s and 20 Hz 80 s) before exposure to alkaline buffer (NH_4Cl). (b) Mean traces displaying the average syHy fluorescent response ($\Delta F/F_0$) of cortical neurons expressing CHMP2B^{Wildtype} (black) and CHMP2B^{Intron5} (orange) are displayed \pm SEM. (c–g) Mean SV pool sizes ($\Delta F/F_0$) for the RRP (c), recycling pool (d), reserve pool (e), resting pool (f) and total SV pool (g) are displayed \pm SEM. For all experiments, $n = 11$ for CHMP2B^{Wildtype} and $n = 8$ for CHMP2B^{Intron5}. Student t-test $*p < 0.05$

4 | DISCUSSION

4.1 | Subneuronal region-specific endolysosomal defects in FTD

Recent studies have shown that FTD causative genes converge on dysfunction of the endolysosomal system. We have recently shown that mutant CHMP2B causes defective neuronal endolysosomal trafficking, leading to a lysosomal storage pathology (Clayton et al., 2015, 2018). However, the molecular mechanism by which defective endolysosomal trafficking specifically causes neuronal dysfunction, rather than global cell death, remains to be described. Neurons are highly compartmentalised cells, with numerous specialised functions, and as such, endolysosomal defects could impact numerous region-specific neuronal functions. We have shown here for the first time how defects in SV membrane trafficking caused by mutation in the ESCRT-III component CHMP2B specifically affect trafficking at the presynaptic terminal, leading to an increase in the number of presynaptic endosomes, defective SV exocytosis, and a retention of

SV-associated proteins in aged mutant CHMP2B mice despite observed synaptic loss.

4.2 | A model for mutant CHMP2B synaptopathy

How do the SV defects lead to a synaptopathy in the mutant CHMP2B FTD model? We propose a model of compromised synaptic protein membrane trafficking because of mutant CHMP2B, with downstream effects on the SV cycle leading to reduced exocytosis, altered vesicle pool dynamics, loss of synapses through down-regulated synaptic transmission and accumulation of SV proteins in the remaining synaptic terminals.

It is clear that resolution of presynaptic endosomes is compromised in mutant CHMP2B neurons. Unstimulated primary cultures of mutant CHMP2B cortical neurons, though from very young animals, already contain more presynaptic endosomes than control cells. Strong stimulation leads to an immediate exacerbation of this accumulation of endosomes in mutant presynaptic terminals as SV



membrane is driven through the membrane recycling and vesicle reformation process. Although we did not detect an immediate effect on the total number of SVs, CHMP2B FTD appears to alter the pool identity of vesicle dynamics, with a significant increase in the total pool of recycling vesicles. This pool contains newly generated SVs (Cheung et al., 2010; Granseth & Lagnado, 2008), and this increase in the total recycling pool of RRP and RP SVs may explain why there is not a large effect on exocytosis in these mutant CHMP2B expressing neurons. This may indicate a compensatory mechanism, with more SVs being mobilised to compensate for the observed exocytic defects. Although no defect was seen in SV endocytosis until the final stimulus of the repeated train, it is possible that endocytosis initially appears unaffected because of the increase in the total recycling SV pool. Reduced exocytosis models the long term depression model of reduced postsynaptic activity driven by reduced presynaptic release, ultimately destabilising the synapse and resulting in loss of the synaptic unit. Clearly, the synapses are able to maintain function for a significant amount of time with this defect; despite exocytic defects, the mutant CHMP2B neurons were able to maintain synaptic turnover during repeated challenges with bursts of action potentials until endocytosis became compromised. Interestingly, although ESCRTs are important for formation of MVBs, no difference was seen in the number of MVBs seen per synapse. However, it should be noted that the incidence of finding a synaptic MVB is extremely low leading to under powering of the comparison.

Although a young-onset dementia, FTD caused by mutant CHMP2B does not present for several decades, indicating that alternative mechanisms may compensate for the reduction in SV protein degradation in the presence of mutant CHMP2B. Whether subtypes of cortical neurons are affected by this change, and how this translates to circuit level changes and behavioural alteration remains to be investigated.

4.3 | Selective retention of presynaptic SV proteins

Several SV proteins specifically are specifically retained in aged mutant CHMP2B mice—Amphiphysin, Endophilin, Synapsin ½ and Synuclein. These proteins are all associated with the trafficking of SVs; Synapsins ½ are SV-associated proteins that modulate neurotransmitter release by tethering SVs to cytoskeletal components (27), while Amphiphysin and Endophilin are BAR domain containing proteins which mediate membrane curvature during endocytosis of SVs from the presynaptic terminal following neurotransmitter release (28–30). Synapsin has been shown to form a distinct liquid phase in an aqueous environment (Milovanovic et al., 2018), and in fact, all of these particular SV-associated proteins have been postulated to be possible phase separation competent proteins (Milovanovic & De, 2017). Aberrant accumulation of phase separation competent proteins could dramatically alter local dynamics, which could ultimately have downstream effects on clustering and mobility of the SV pool.

Not all investigated SV-associated proteins were retained in aged mutant CHMP2B mice. Synaptophysin and Synaptotagmin were not

retained in mutant CHMP2B mice compared to controls (Figure S5), indicating selectivity in the degradative role of ESCRTs at the presynaptic terminal. Indeed, other studies have also shown selective degradation of SV proteins. A subset of SV proteins were found to be degraded in a Rab35 and ESCRT activity-dependent mechanism (Sheehan et al., 2016). Additionally TBC1D24, mutations in which cause severe epilepsy and neurodegeneration, is important for the lysosomal trafficking of SV proteins and integrity of synaptic transmission (Fernandes et al., 2014). Our observation that SV proteins accumulate selectively in mutant CHMP2B mice provides further evidence that different SV proteins may be degraded by distinct degradative mechanisms. This evidence supports the theory that SVs are not discretely degraded as a quantal unit, but that a subset of SV proteins is trafficked via the presynaptic endosome for ESCRT dependent degradation.

4.4 | SV trafficking dysfunction in dementia

Numerous protein networks and signalling cascades contribute to ensure the tight regulation of SV trafficking. Several proteins associated with neurodegenerative disease have been implicated in the SV cycle, suggesting that disruption of this highly tuned SV cycle precedes synapse loss and eventual neurodegeneration in several dementias. For example, α -synuclein over-expression or mutation is associated with several dementias, including Parkinson's disease, Lewy body dementia, multiple system atrophy and some variants of AD. Although the specific physiological role of α -synuclein is not yet well understood, disruption of α -synuclein is associated with defects in SV cycling (Cabin et al., 2002; Fusco et al., 2016; Scott & Roy, 2012; Wang et al., 2014).

The recently published observations that the FTD associated proteins progranulin, tau and C9orf72 have all been found at the presynaptic terminal raises the possibility that presynaptic endolysosomal defects impact SV trafficking in numerous genetic forms of FTD (Frick et al., 2018; Petoukhov et al., 2013; Zhou et al., 2017). Supporting this possibility, pathogenic tau has recently been shown to alter presynaptic functions through binding with SVs and reducing their mobility and release rate (Zhou et al., 2017). Additionally, glycine-alanine dipeptides associated with C9orf72 mutation have recently been shown to alter SV fusion in neurons expressing GFP tagged glycine-alanine dipeptides (Jensen et al., 2020).

4.5 | CHMP2B FTD is a novel synaptopathy with a novel mechanism

Defective SV protein degradation may lead to several knock-on effects at both the cellular and the circuit level in mutant CHMP2B mice. Of particular interest would be the downstream effect on neurotransmission and ultimately on neuronal circuits in areas of the brain affected. Behavioural deficits are not seen in this mouse model until 18 months of age, when neuron loss is well established (Clayton



et al., 2017), indicating that homeostatic mechanisms may be able to compensate for initial synaptopathy. In agreement with this, brain array tomography in the Tg4510 mouse model of tauopathy has shown that tau induced loss of a subset of synapses may be initially compensated for by increase in other synapse subtypes (Kopeikina et al., 2013), which may explain why synaptic protein levels were not found to be altered at 6 months in mutant CHMP2B mice.

Our data showing that FTD causative mutant CHMP2B causes defective SV trafficking, and the convergence of several distinct neurodegenerative proteins on the SV pathway suggests that defects in SV trafficking are an important and early event in neurodegenerative pathogenesis. This warrants further mechanistic investigation in terms of potential therapeutic targets, in particular, the pathways responsible for sustained presynaptic performance in mutant CHMP2B provide promise as a route to increase synaptic resilience.

ETHICS APPROVAL AND CONSENT TO PARTICIPATE

All mouse work was performed in accordance with the ethical standards laid down in the Animals (Scientific Procedures) Act 1986, UK.

ACKNOWLEDGEMENTS

We thank Kerri Venner for technical support with electron microscopy.

CONFLICT OF INTEREST

Michael A. Cousin is an editor for the Journal of Neurochemistry. No other authors have any conflicts of interest to declare.

AUTHOR CONTRIBUTIONS

ELC conceived the study. ELC designed the study. ELC, MAC, AMI and SS obtained funding. AMI provided materials. ELC and KB performed experiments. ELC and KB analysed data. ELC, KB, MAC and SS interpreted data. ELC and MAC wrote the manuscript. ELC, KB, AMI, MAC and SS edited the manuscript. All authors read and approved the final manuscript.

DATA AVAILABILITY STATEMENT

Raw data is available from the corresponding author upon request.

ORCID

Emma L. Clayton  <https://orcid.org/0000-0003-0937-2874>

Katherine Bonnycastle  <https://orcid.org/0000-0002-3393-5625>

Michael A. Cousin  <https://orcid.org/0000-0002-1762-160X>

Stephanie Schorge  <https://orcid.org/0000-0003-1541-5148>

REFERENCES

- Atluri, P. P., & Ryan, T. A. (2006). The kinetics of synaptic vesicle reacidification at hippocampal nerve terminals. *Journal of Neuroscience*, 26, 2313–2320. <https://doi.org/10.1523/JNEUROSCI.4425-05.2006>
- Bonnycastle, K., Davenport, E. C., & Cousin, M. A. (2020). Presynaptic dysfunction in neurodevelopmental disorders: Insights from the synaptic vesicle life cycle. *Journal of Neurochemistry*. <https://doi.org/10.1111/jnc.15035>
- Cabin, D. E., Shimazu, K., Murphy, D., Cole, N. B., Gottschalk, W., McIlwain, K. L., Orrison, B., Chen, A., Ellis, C. E., Paylor, R., Lu, B., & Nussbaum, R. L. (2002). Synaptic vesicle depletion correlates with attenuated synaptic responses to prolonged repetitive stimulation in mice lacking alpha-synuclein. *Journal of Neuroscience*, 22, 8797–8807.
- Chanaday, N. L., Cousin, M. A., Milosevic, I., Watanabe, S., & Morgan, J. R. (2019). The synaptic vesicle cycle revisited: New insights into the modes and mechanisms. *Journal of Neuroscience*, 39, 8209–8216. <https://doi.org/10.1523/JNEUROSCI.1158-19.2019>
- Cheung, G., Jupp, O. J., & Cousin, M. A. (2010). Activity-dependent bulk endocytosis and clathrin-dependent endocytosis replenish specific synaptic vesicle pools in central nerve terminals. *Journal of Neuroscience*, 30, 8151–8161. <https://doi.org/10.1523/JNEUROSCI.0293-10.2010>
- Clayton, E. L., Anggono, V., Smillie, K. J., Chau, N., Robinson, P. J., & Cousin, M. A. (2009). The phospho-dependent dynamin-syndapin interaction triggers activity-dependent bulk endocytosis of synaptic vesicles. *Journal of Neuroscience*, 29, 7706–7717. <https://doi.org/10.1523/JNEUROSCI.1976-09.2009>
- Clayton, E. L., Evans, G. J., & Cousin, M. A. (2008). Bulk synaptic vesicle endocytosis is rapidly triggered during strong stimulation. *Journal of Neuroscience*, 28, 6627–6632. <https://doi.org/10.1523/JNEUROSCI.1445-08.2008>
- Clayton, E. L., Mancuso, R., Nielsen, T. T., Mizielinska, S., Holmes, H., Powell, N., Norona, F., Overgaard, L. J., Milioto, C., Wilson, K. M., Lythgoe, M. F., Ourselin, S., Nielsen, J. E., Johannsen, P., Holm, I., Collinge, J., Frej, A., Oliver, P. L., Gomez-Nicola, D., & Isaacs, A. M. (2017). Early microgliosis precedes neuronal loss and behavioural impairment in mice with a frontotemporal dementia-causing CHMP2B mutation. *Human Molecular Genetics*, 26(5), 873–887.
- Clayton, E. L., Milioto, C., Muralidharan, B., Norona, F. E., Edgar, J. R., Soriano, A., Jafar-Nejad, P., Rigo, F., Collinge, J., & Isaacs, A. M. (2018). Frontotemporal dementia causative CHMP2B impairs neuronal endolysosomal traffic-rescue by TMEM106B knockdown. *Brain*, 141, 3428–3442.
- Clayton, E. L., Mizielinska, S., Edgar, J. R., Nielsen, T. T., Marshall, S., Norona, F. E., Robbins, M., Damirji, H., Holm, I. E., Johannsen, P., Nielsen, J. E., Asante, E. A., Collinge, J., & Isaacs, A. M. (2015). Frontotemporal dementia caused by CHMP2B mutation is characterised by neuronal lysosomal storage pathology. *Acta Neuropathologica*, 130, 511–523. <https://doi.org/10.1007/s00401-015-1475-3>
- Clayton, E. L., Sue, N., Smillie, K. J., O'Leary, T., Bache, N., Cheung, G., Cole, A. R., Wyllie, D. J., Sutherland, C., Robinson, P. J., & Cousin, M. A. (2010). Dynamin I phosphorylation by GSK3 controls activity-dependent bulk endocytosis of synaptic vesicles. *Nature Neuroscience*, 13, 845–851.
- Dekosky, S. T., & Scheff, S. W. (1990). Synapse loss in frontal cortex biopsies in Alzheimer's disease: correlation with cognitive severity. *Annals of Neurology*, 27, 457–464. <https://doi.org/10.1002/ana.410270502>
- Egashira, Y., Takase, M., & Takamori, S. (2015). Monitoring of vacuolar-type H⁺ ATPase-mediated proton influx into synaptic vesicles. *Journal of Neuroscience*, 35, 3701–3710. <https://doi.org/10.1523/JNEUROSCI.4160-14.2015>
- Fernandes, A. C., Uytterhoeven, V., Kuenen, S., Wang, Y. C., Slabbaert, J. R., Swerts, J., Kasprovicz, J., Aerts, S., & Verstreken, P. (2014). Reduced synaptic vesicle protein degradation at lysosomes curbs TBC1D24/sky-induced neurodegeneration. *Journal of Cell Biology*, 207, 453–462. <https://doi.org/10.1083/jcb.201406026>
- Ferrer, I. (1999). Neurons and their dendrites in frontotemporal dementia. *Dementia and Geriatric Cognitive Disorders*, 10(Suppl 1), 55–60.
- Frick, P., Sellier, C., Mackenzie, I. R. A., Cheng, C. Y., Tahraoui-Bories, J., Martinat, C., Pasterkamp, R. J., Prudlo, J., Edbauer, D., Oulad-Abdelghani, M., Feederle, R., Charlet-Berguerand, N., & Neumann, M. (2018). Novel antibodies reveal presynaptic localization of



- C9orf72 protein and reduced protein levels in C9orf72 mutation carriers. *Acta Neuropathologica Communications*, 6, 72.
- Fusco, G., Pape, T., Stephens, A. D., Mahou, P., Costa, A. R., Kaminski, C. F., Kaminski, S. G., Schierle, G. S., Vendruscolo, M., Veglia, G., Dobson, C. M., & De Simone, A. (2016). Structural basis of synaptic vesicle assembly promoted by alpha-synuclein. *Nature Communications*, 7, 12563.
- Gascon, E., Lynch, K., Ruan, H., Almeida, S., Verheyden, J. M., Seeley, W. W., Dickson, D. W., Petrucelli, L., Sun, D., Jiao, J., Zhou, H., Jakovcevski, M., Akbarian, S., Yao, W. D., & Gao, F. B. (2014). Alterations in microRNA-124 and AMPA receptors contribute to social behavioral deficits in frontotemporal dementia. *Nature Medicine*, 20, 1444–1451.
- Ghazi-Noori, S., Froud, K. E., Mizielinska, S., Powell, C., Smidak, M., Fernandez de Marco, M., O'Malley, C., Farmer, M., Parkinson, N., Fisher, E. M. C., Asante, E. A., Brandner, S., Collinge, J., & Isaacs, A. M. (2012). Progressive neuronal inclusion formation and axonal degeneration in CHMP2B mutant transgenic mice. *Brain*, 135, 819–832. <https://doi.org/10.1093/brain/aws006>
- Gijssels, I., Van, M. S., van der Zee, J., Sieben, A., Philtjens, S., Heeman, B., Engelborghs, S., Vandenbuerck, M., De, B. G., Baumer, V., Cuijt, I., Van den Broeck, M., Peeters, K., Mattheijssens, M., Rousseau, F., Vandenbergh, R., De, J. P., Cras, P., De Deyn, P. P., ... Van, B. C. (2015). Loss of TBK1 is a frequent cause of frontotemporal dementia in a Belgian cohort. *Neurology*, 85, 2116–2125.
- Granseth, B., & Lagnado, L. (2008). The role of endocytosis in regulating the strength of hippocampal synapses. *Journal of Physiology*, 586, 5969–5982. <https://doi.org/10.1113/jphysiol.2008.159715>
- Harvey, R. J., Skelton-Robinson, M., & Rossor, M. N. (2003). The prevalence and causes of dementia in people under the age of 65 years. *Journal of Neurology, Neurosurgery and Psychiatry*, 74, 1206–1209.
- Jensen, B. K., Schuldi, M. H., McAvoy, K., Russell, K. A., Boehringer, A., Curran, B. M., Krishnamurthy, K., Wen, X., Westergard, T., Ma, L., Haeusler, A. R., Edbauer, D., Pasinelli, P., & Trotti, D. (2020). Synaptic dysfunction induced by glycine-alanine dipeptides in C9orf72-ALS/FTD is rescued by SV2 replenishment. *EMBO Molecular Medicine*, 12, e10722.
- Kavalali, E. T., & Jorgensen, E. M. (2014). Visualizing presynaptic function. *Nature Neuroscience*, 17, 10–16.
- Kavanagh, D. M., Smyth, A. M., Martin, K. J., Dun, A., Brown, E. R., Gordon, S., Smillie, K. J., Chamberlain, L. H., Wilson, R. S., Yang, L., Lu, W., Cousin, M. A., Rickman, C., & Duncan, R. R. (2014). A molecular toggle after exocytosis sequesters the presynaptic syntaxin1a molecules involved in prior vesicle fusion. *Nature Communications*, 5, 5774.
- Kim, S. H., & Ryan, T. A. (2010). CDK5 serves as a major control point in neurotransmitter release. *Neuron*, 67, 797–809. <https://doi.org/10.1016/j.neuron.2010.08.003>
- Kononenko, N. L., Puchkov, D., Classen, G. A., Walter, A. M., Pechstein, A., Sawade, L., Kaempf, N., Trimbuch, T., Lorenz, D., Rosenmund, C., Maritzen, T., & Haucke, V. (2014). Clathrin/AP-2 mediate synaptic vesicle reformation from endosome-like vacuoles but are not essential for membrane retrieval at central synapses. *Neuron*, 82, 981–988. <https://doi.org/10.1016/j.neuron.2014.05.007>
- Kopeikina, K. J., Wegmann, S., Pitstick, R., Carlson, G. A., Bacskai, B. J., Betensky, R. A., Hyman, B. T., & Spire-Jones, T. L. (2013). Tau causes synapse loss without disrupting calcium homeostasis in the rTg4510 model of tauopathy. *PLoS One*, 8, e80834. <https://doi.org/10.1371/journal.pone.0080834>
- Le Ber, I., De, S. A., Millicamps, S., Camuzat, A., Caroppo, P., Couratier, P., Blanc, F., Lacomblez, L., Sellal, F., Fleury, M. C., Meininger, V., Cazeneuve, C., Clot, F., Flabeau, O., LeGuern, E., & Brice, A. (2015). TBK1 mutation frequencies in French frontotemporal dementia and amyotrophic lateral sclerosis cohorts. *Neurobiology of Aging*, 36, 3116–3118.
- Lindquist, S. G., Braedgaard, H., Svenstrup, K., Isaacs, A. M., & Nielsen, J. E. (2008). Frontotemporal dementia linked to chromosome 3 (FTD-3)—current concepts and the detection of a previously unknown branch of the Danish FTD-3 family. *European Journal of Neurology*, 15, 667–670. <https://doi.org/10.1111/j.1468-1331.2008.02144.x>
- Liu, X., Erikson, C., & Brun, A. (1996). Cortical synaptic changes and gliosis in normal aging, Alzheimer's disease and frontal lobe degeneration. *Dementia*, 7, 128–134.
- McKhann, G. M., Albert, M. S., Grossman, M., Miller, B., Dickson, D., & Trojanowski, J. Q. (2001). Clinical and pathological diagnosis of frontotemporal dementia: report of the Work Group on Frontotemporal Dementia and Pick's Disease. *Archives of Neurology*, 58, 1803–1809. <https://doi.org/10.1001/archneur.58.11.1803>
- Melland, H., Carr, E. M., & Gordon, S. L. (2020). Disorders of synaptic vesicle fusion machinery. *Journal of Neurochemistry*, 157(2), 130–164. <https://doi.org/10.1111/jnc.15181>
- Milovanovic, D., & De, C. P. (2017). Synaptic vesicle clusters at synapses: A distinct liquid phase? *Neuron*, 93, 995–1002. <https://doi.org/10.1016/j.neuron.2017.02.013>
- Milovanovic, D., Wu, Y., Bian, X., & De, C. P. (2018). A liquid phase of synapsin and lipid vesicles. *Science*, 361, 604–607. <https://doi.org/10.1126/science.aat5671>
- Mucke, L., Masliah, E., Yu, G. Q., Mallory, M., Rockenstein, E. M., Tatsuno, G., Hu, K., Kholodenko, D., Johnson-Wood, K., & McConlogue, L. (2000). High-level neuronal expression of abeta 1–42 in wild-type human amyloid protein precursor transgenic mice: synaptotoxicity without plaque formation. *Journal of Neuroscience*, 20, 4050–4058.
- Neary, D., Snowden, J. S., Gustafson, L., Passant, U., Stuss, D., Black, S., Freedman, M., Kertesz, A., Robert, P. H., Albert, M., Boone, K., Miller, B. L., Cummings, J., & Benson, D. F. (1998). Frontotemporal lobar degeneration: A consensus on clinical diagnostic criteria. *Neurology*, 51, 1546–1554. <https://doi.org/10.1212/WNL.51.6.1546>
- Nicholson-Fish, J. C., Kokotos, A. C., Gillingwater, T. H., Smillie, K. J., & Cousin, M. A. (2015). VAMP4 is an essential cargo molecule for activity-dependent bulk endocytosis. *Neuron*, 88, 973–984. <https://doi.org/10.1016/j.neuron.2015.10.043>
- Petoukhov, E., Fernando, S., Mills, F., Shivji, F., Hunter, D., Krieger, C., Silverman, M. A., & Bamji, S. X. (2013). Activity-dependent secretion of progranulin from synapses. *Journal of Cell Science*, 126, 5412–5421. <https://doi.org/10.1242/jcs.132076>
- Pottier, C., Bieniek, K. F., Finch, N. C., van de Vorst, M., Baker, M., Perkersen, R., Brown, P., Ravenscroft, T., van Blitterswijk, M., Nicholson, A. M., DeTure, M., Knopman, D. S., Josephs, K. A., Parisi, J. E., Petersen, R. C., Boylan, K. B., Boeve, B. F., Graff-Radford, N. R., Veltman, J. A., ... Rademakers, R. (2015). Whole-genome sequencing reveals important role for TBK1 and OPTN mutations in frontotemporal lobar degeneration without motor neuron disease. *Acta Neuropathologica*, 130, 77–92. <https://doi.org/10.1007/s00401-015-1436-x>
- Ratnavalli, E., Brayne, C., Dawson, K., & Hodges, J. R. (2002). The prevalence of frontotemporal dementia. *Neurology*, 58, 1615–1621. <https://doi.org/10.1212/WNL.58.11.1615>
- Rohrer, J. D., & Warren, J. D. (2011). Phenotypic signatures of genetic frontotemporal dementia. *Current Opinion in Neurology*, 24, 542–549.
- Sankaranarayanan, S., & Ryan, T. A. (2001). Calcium accelerates endocytosis of vSNAREs at hippocampal synapses. *Nature Neuroscience*, 4, 129–136.
- Scott, D., & Roy, S. (2012). alpha-Synuclein inhibits intersynaptic vesicle mobility and maintains recycling-pool homeostasis. *Journal of Neuroscience*, 32, 10129–10135. <https://doi.org/10.1523/JNEUROSCI.0535-12.2012>
- Serrano-Pozo, A., Frosch, M. P., Masliah, E., & Hyman, B. T. (2011). Neuropathological alterations in Alzheimer disease. *Cold Spring Harbor Perspectives in Medicine*, 1, a006189. <https://doi.org/10.1101/cshperspect.a006189>



- Sheehan, P., Zhu, M., Beskow, A., Vollmer, C., & Waites, C. L. (2016). Activity-dependent degradation of synaptic vesicle proteins requires Rab35 and the ESCRT pathway. *Journal of Neuroscience*, 36, 8668–8686. <https://doi.org/10.1523/JNEUROSCI.0725-16.2016>
- Sheng, M., Sabatini, B. L., & Südhof, T. C. (2012). Synapses and Alzheimer's disease. *Cold Spring Harbor Perspectives in Biology*, 4(5), a005777.
- Skibinski, G., Parkinson, N. J., Brown, J. M., Chakrabarti, L., Lloyd, S. L., Hummerich, H., Nielsen, J. E., Hodges, J. R., Spillantini, M. G., Thusgaard, T., Brandner, S., Brun, A., Rossor, M. N., Gade, A., Johannsen, P., Sorensen, S. A., Gydesen, S., Fisher, E. M., & Collinge, J. (2005). Mutations in the endosomal ESCRTIII-complex subunit CHMP2B in frontotemporal dementia. *Nature Genetics*, 37, 806–808.
- Südhof, T. C. (2013). Neurotransmitter release: the last millisecond in the life of a synaptic vesicle. *Neuron*, 80, 675–690. <https://doi.org/10.1016/j.neuron.2013.10.022>
- Terry, R. D. (2000). Cell death or synaptic loss in Alzheimer disease. *Journal of Neuropathology and Experimental Neurology*, 59, 1118–1119.
- Terry, R. D., Masliah, E., Salmon, D. P., Butters, N., DeTeresa, R., Hill, R., Hansen, L. A., & Katzman, R. (1991). Physical basis of cognitive alterations in Alzheimer's disease: Synapse loss is the major correlate of cognitive impairment. *Annals of Neurology*, 30, 572–580. <https://doi.org/10.1002/ana.410300410>
- van der Zee, J., Gijssels, I., Van, M. S., Perrone, F., Dillen, L., Heeman, B., Baumer, V., Engelborghs, S., De, B. J., Baets, J., Gelpi, E., Rojas-Garcia, R., Clarimon, J., Lleó, A., Diehl-Schmid, J., Alexopoulos, P., Pernecky, R., Synofzik, M., Just, J., ... Testi, S. (2017). TBK1 mutation spectrum in an extended European patient cohort with frontotemporal dementia and amyotrophic lateral sclerosis. *Human Mutation*, 38, 297–309.
- Vietri, M., Radulovic, M., & Stenmark, H. (2020). The many functions of ESCRTs. *Nature Reviews Molecular Cell Biology*, 21, 25–42.
- Wang, L., Das, U., Scott, D. A., Tang, Y., McLean, P. J., & Roy, S. (2014). alpha-Synuclein multimers cluster synaptic vesicles and attenuate recycling. *Current Biology*, 24, 2319–2326.
- Watanabe, S., Trimbuch, T., Camacho-Pérez, M., Rost, B. R., Brokowski, B., Söhl-Kielczynski, B., Felies, A., Davis, M. W., Rosenmund, C., & Jorgensen, E. M. (2014). Clathrin regenerates synaptic vesicles from endosomes. *Nature*, 515, 228–233. <https://doi.org/10.1038/nature13846>
- Zhou, L., McInnes, J., Wierda, K., Holt, M., Herrmann, A. G., Jackson, R. J., Wang, Y. C., Swerts, J., Beyens, J., Miskiewicz, K., Vilain, S., Dewachter, I., Moechars, D., De, S. B., Spiess-Jones, T. L., De, W. J., & Verstreken, P. (2017). Tau association with synaptic vesicles causes presynaptic dysfunction. *Nature Communications*, 8, 15295.

SUPPORTING INFORMATION

Additional supporting information may be found in the online version of the article at the publisher's website.

How to cite this article: Clayton, E. L., Bonnycastle, K., Isaacs, A. M., Cousin, M. A., & Schorge, S. (2022). A novel synaptopathy-defective synaptic vesicle protein trafficking in the mutant CHMP2B mouse model of frontotemporal dementia. *Journal of Neurochemistry*, 160, 412–425. <https://doi.org/10.1111/jnc.15551>